Thermal Ignition Phenomena in Chain-Addition Copolymerizations

D. H. SEBASTIAN and J. A. BIESENBERGER, *Department of Chemistry and Chemical Engineering, Stevens Institute of Technology, Hoboken, New Jersey 07030*

Synopsis

Thermal ignition theory has been extended to include free-radical copolymerizations resulting in dimensionless criteria for runaway and ignition. These criteria were verified by computer simulation and preliminary experimentation. Approximate, but greatly simplified, material and energy balances describing nonisothermal copolymerizations were developed which are similar in form to those describing nonisothermal homopolymerizations. Regions of close agreement, as well as disagreement, between conversion and temperature histories from these approximations and those from the exact balances are described.

INTRODUCTION

This work is concerned with nonuniform temperature in chain-addition copolymerizations, and especially with the phenomenon frequently termed thermal runaway (R-A). Thermal runaway has been defined in a previous paper on homopolymerizations[1] as a reaction with temperature profile $T(t)$ having upward concavity. Potentially unstable R-A, or thermal ignition (IG), has thus been defined as parametrically sensitive R-A.

Our earlier work on homopolymerizations[1-4] combined a Semenov-type analysis with computer simulations and resulted in dimensionless criteria in terms of parameter groupings which characterized R-A and IG in chain-addition polymerizations. These criteria are

$$a < 2 \tag{1}$$

$$B > 20 \tag{2}$$

$$b > 100 \tag{3}$$

where dimensionless groups, a, B, and b are defined in the text. Thus, R-A occurs when inequality (1) is satisifed and IG, when inequalities (2) and (3) are additionally satisifed.

Graphical IG boundaries were generated, similar to the familiar explosion-limit curves for explosive gases, which spanned a wide range of values for the above and other pertinent parameters typical of many common free radical-type monomer–initiator systems. The system styrene–benzoyl peroxide (S/BP) was used to verify predicted R-A and IG behavior experimentally.[4] Laboratory data demonstrated that key dimensionless groupings successfully predicted R-A and R-A transitions and defined regions of disappearing R-A sensitivity. Experi-

Journal of Applied Polymer Science, Vol. 23, 661–686 (1979)

0021/8995/79/0023-0661$01.00

TABLE I
Elementary Kinetic Steps

Initiation

$$m_0 \xrightarrow{k_d} R^* \qquad \text{or} \qquad I \xrightarrow{k_d} 2R^*$$

$$R^* + A \xrightarrow{k_{i1}} A^* \qquad R^* + B \xrightarrow{k_{i2}} B^*$$

Propagation

$$k_{pii}\begin{cases} -A^* + A \xrightarrow{k_{p11}} -AA^* \\ -B^* + B \xrightarrow{k_{p22}} -BB^* \end{cases} \qquad k_{pij}\begin{cases} -A^* + B \xrightarrow{k_{p12}} -AB^* \\ -B^* + A \xrightarrow{k_{p21}} -BA^* \end{cases}$$

Termination

Ultimate effect (geometric mean and phi-factor)

$$k_{tii}\begin{cases} -A^* + {}^*A- \xrightarrow{k_{t11}} \\ -B^* + {}^*B- \xrightarrow{k_{t22}} \end{cases} \qquad k_{tij}\ -A^* + {}^*B- \xrightarrow{k_{t12}}$$

Penultimate effect

$$k_{tiiii}\begin{cases} -AA^* + {}^*AA- \xrightarrow{k_{t1111}} \\ -BB^* + {}^*BB- \xrightarrow{k_{t2222}} \end{cases} \qquad k_{tijji}\begin{cases} -AB^* + {}^*BA- \xrightarrow{k_{t1221}} \\ -BA^* + {}^*AB- \xrightarrow{k_{t2112}} \end{cases}$$

$$k_{tiiij}\begin{cases} -AA^* + {}^*AB- \xrightarrow{k_{t1112}} \\ -BB^* + {}^*BA- \xrightarrow{k_{t2221}} \end{cases} \qquad k_{tiiji}\begin{cases} -AA^* + {}^*BA- \xrightarrow{k_{t1121}} \\ -BB^* + {}^*AB- \xrightarrow{k_{t2212}} \end{cases}$$

$$k_{tiijj}\ -AA^* + {}^*BB- \xrightarrow{k_{t1122}} \qquad k_{tijij}\ -AB^* + {}^*AB- \xrightarrow{k_{t1212}}$$

mental IG boundaries, determined at several levels of initiator concentration, showed close agreement with semitheoretical boundaries.

The present paper attempts to analyze in a general way the R-A behavior of chain-addition copolymerizations, which are complicated by problems of composition drift and obscure kinetic mechanisms, in addition to degree of polymerization drift. It may thus be viewed as a sequel to reference 1. In subsequent papers[5,6] we shall present the results of numerous computer simulation studies and experiments.

KINETIC MODEL

As with our earlier work on homopolymerizations, we have found that kinetic phenomena such as chain transfer, gel effect, thermal initiation, etc., while important factors in determining the properties of polymer products, play only a small role in shaping the entire thermal trajectory of polymerizations and have

TABLE II
Rate Functions

Initiation

$$R_{i1} = k_i f_1[m_0] \qquad R_{i2} = k_i f_2[m_0]$$

where for free-radical polymerizations

$$k_i = fk_d \qquad f = \text{efficiency factor, see reference (8)}$$

$$[m_0] = 2[I]$$

$$f_1 \equiv k_{i1}[A]/(k_{i1}[A] + k_{i2}[B])$$

$$f_2 = 1 - f_1$$

$$R_i = R_{i1} + R_{i2} = k_i[m_0] = 2fk_d[\mathrm{I}]$$

Propagation

$$R_{p1} = R_{p11} + R_{p21} = k_{p11}[A^*][A] + k_{p21}[B^*][A]$$

$$R_{p2} = R_{p22} + R_{p12} = k_{p22}[B^*][B] + k_{p12}[A^*][B]$$

where

$$[A^*] \equiv [AA^*] + [BA^*]$$

$$[B^*] \equiv [BB^*] + [AB^*]$$

QSSA leads to symmetry:

$$R_{p12} = R_{p21} \text{ or } k_{p12}[A^*][B] = k_{p21}[B^*][A]$$

$$R_p = R_{p1} + R_{p2} = k_{p11}[A^*][A] + 2k_{p12}[A^*][B] + k_{p22}[B^*][B]$$

Termination

Ultimate effect (geometric mean and phi-factor):

$$R_t = k_{t11}[A^*]^2 + 2k_{t12}[A^*][B^*] + k_{t22}[B^*]^2$$

Penultimate effect:

$$R_t = k_{t1111}[AA^*]^2 + k_{t2112}[BA^*]^2 + 2k_{t1112}[AA^*][BA^*] + 2k_{t1121}[AA^*][BB^*] + 2k_{t2121}[BA^*][AB^*] + 2k_{t2212}[BB^*][BA^*] + 2k_{t2221}[BB^*][AB^*] + k_{t1221}[AB^*]^2 + k_{t2222}[BB^*]^2$$

Special case: reduces to ultimate effect case

when $k_{tijkl} \boxdot k_{tjk} = k_{tkj}$ for $i = 1$ or 2, $j = 1$ or 2, $k = 1$ or 2, and $l = 1$ or 2

virtually no effect on the characterization of R-A and IG, per se, based upon the most elementary steps of initiation, propagation, and termination. We thus eliminate them from consideration here as we have done earlier.[1–4]

The kinetic steps used and associated rate functions are detailed in Tables I and II. The rate of initiator decomposition was assumed to be the same in either comonomer. Thus, the rate of initiation is independent of comonomer composition. While the propagation steps are generally agreed upon, the termination process is as yet not fully understood. Several models have appeared in the literature[7–16] which reproduce experimental rate data with varying degrees of success. In the earliest treatment,[7] it was presumed that termination rates depended only upon terminal groups on reacting radicals. Homopolymerization rate constants were thus applied to termination of like radicals during copoly-

TABLE III
Termination Models

Geometric Mean Model

$$k_{tij} = (k_{tii}k_{tjj})^{1/2} = k_{tji}$$

NOTE: two independent constants, k_{tii} for $i = 1$ or 2

$$R_t = (k_{t11}{}^{1/2}[A^*] + k_{t22}{}^{1/2}[B^*])^2$$

Phi-Factor Model

$$\varphi \equiv k_{tij}/(k_{tii}k_{tjj})^{1/2} = k_{tji}(k_{tii}k_{tjj})^{1/2}$$

NOTE: two independent constants, k_{tii} for $i = 1$ or 2

$$R_t = k_{t11}[A^*]^2 + 2\varphi(k_{t11}k_{t22})^{1/2}[A^*][B^*] + k_{t22}[B^*]^2$$

Special case $\varphi = 1$:

$$R_t = (k_{t11}{}^{1/2}[A^*] + k_{t22}{}^{1/2}[B^*])^2$$

Penultimate Effect Model

$$k_{tiiij} = (k_{tiiii}k_{tjiij})^{1/2} = k_{tijii}$$

$$k_{tiiij} = (k_{tiiii}k_{tjjjj})^{1/2} = k_{tjjii}$$

$$k_{tiiji} = (k_{tiiii}k_{tijji})^{1/2} = k_{tjiii}$$

$$k_{tijij} = (k_{tijji}k_{tjiij})^{1/2} = k_{tjiji}$$

NOTE: four independent constants, k_{tiiii} and k_{tijji} for $i = 1$ or 2, $j = 1$ or 2, and $i \neq j$

$$R_t = (k_{t1111}{}^{1/2}[AA^*] + k_{t1221}{}^{1/2}[AB^*] + k_{t2112}{}^{1/2}[BA^*] + k_{t2222}[BB^*])^2$$

Special case $k_{tijji} = k_{tiiii}$

$$R_t = (k_{t1111}{}^{1/2}[A^*] + k_{t2222}{}^{1/2}[B^*]^2) \equiv (k_{t11}{}^{1/2}[A^*] + k_{t22}{}^{1/2}[B^*])^2$$

merization. On statistical grounds it has been argued that cross-termination rate constants should be the geometric mean of the two homopolymerization constants[8]:

$$k_{t12} = (k_{t11}k_{t22})^{1/2} \tag{4}$$

While satisfactory for styrene–α-methylstyrene copolymerization, this approach was found to be inadequate in describing many other systems.

It was subsequently postulated that polar effects might tend to influence the cross-termination reaction beyond the mere statistical probability that the unlike radicals meet and react. A constant phi-factor was introduced to modify the geometric mean[7,9]:

$$k_{t12} = \varphi(k_{t11}k_{t22})^{1/2} \tag{5}$$

where $\varphi > 1$ indicates a favored cross termination. Rate data for many systems were reproduced with this simple modification. It was found to be particularly useful for the system styrene–methyl methacrylate with $\varphi = 13$. For other systems, however, it was found necessary to vary φ over a wide range of values with varying comonomer feed compositions. For example, φ took on values between 10 and 150 in order to reproduce initial rate data for the system styrene–butyl acrylate. Variations of φ with temperature have not as yet been considered.

TABLE IV
Expressions for Active Intermediates

$$[A^*] = k_{p21}(R_i/k_{t11}k_{t22})^{1/2}[A]H \qquad [B^*] = k_{p12}(R_i/k_{t11}k_{t22})^{1/2}[B]H$$

Geometric Mean

$$H = \left[\frac{k_{p21}[A]}{(k_{t22})^{1/2}} + \frac{k_{p12}[B]}{(k_{t11})^{1/2}}\right]^{-1}$$

Phi-Factor

$$H = \left\{\left[\frac{k_{p21}[A]}{(k_{t22})^{1/2}}\right]^2 + 2\varphi\,\frac{k_{p21}k_{p12}[A][B]}{(k_{t22}k_{t11})^{1/2}} + \left[\frac{k_{p12}[B]}{(k_{t11})^{1/2}}\right]^2\right\}^{-1/2}$$

Penultimate Effect

$$H = \left\{\frac{k_{p21}[A]}{(k_{t22})^{1/2}}\left[\frac{r_1[A] + (k_{t21}/k_{t11})^{1/2}[B]}{r_1[A] + [B]}\right] + \frac{k_{p12}[B]}{(k_{t11})^{1/2}}\left[\frac{r_2[B] + (k_{t12}/k_{t22})^{1/2}[A]}{r_2[B] + [A]}\right]\right\}^{-1}$$

where

$$k_{t11} = k_{t1112}$$

$$k_{t21} = k_{t2112}$$

$$k_{t12} = k_{t1221}$$

$$k_{t22} = k_{t2222}$$

Many researchers have argued[10–14] that the copolymer termination process is diffusion controlled. Several[10,13] have proposed expressions for rate constants as function of the composition of unreacted comonomers. Thus, the "constants" would not only vary with feed composition but would drift with changes in comonomer composition during the course of reaction.

Most recently, the penultimate-effect model was proposed.[14] This model does not attempt to resolve the question of chemical versus diffusion control. It is generally agreed that segmental diffusion of chain ends is the rate-limiting step when termination is diffusion controlled. The penultimate-effect model postulates that the polar and steric characteristics of a chemically controlled termination process depend upon the nature of the last four carbon–carbon bonds in each chain involved. Thus, for vinyl comonomers with two carbon atoms per repeat unit, ten termination steps are distinguishable. They appear in Table I. All termination rate constants may be expressed in terms of four independent k_t values for those reactions in which the ultimate and penultimate repeat units of both active intermediates are identical, as shown in Table III. The development of termination rate expressions for all modes of termination previously discussed is summarized in Tables II and III. We note that with the appropriate assumptions all expressions reduce to those for the geometric mean.

Rate functions for termination, R_t, are needed in the kinetic modeling of copolymerizations when applying the quasi-stationary state approximation (QSSA), $R_i = R_t$, to eliminate concentration terms for active intermediates [A*] and [B*] in the rate equations, just as they are in modeling homopolymerizations. By applying the QSSA to the total population of intermediates (as above) and to the population of each kind of intermediate as well (symmetry condition in Table II), we obtain the expressions for the concentration of each intermediate shown in Table IV for the three termination models discussed.

TABLE V
Rate Functions and Balance Equations for Copolymerizations

Rate Functions for Propagation

$$R_{p11} = k_{p11}k_{p21}(fk_d/k_{t11}k_{t22})^{1/2}[m_1]^2[m_0]^{1/2}H$$

$$R_{p12} = k_{p12}k_{p21}(fk_d/k_{t11}k_{t22})^{1/2}[m_1][m_2][m_0]^{1/2}H = R_{p21}$$

$$R_{p22} = k_{p22}k_{p12}(fk_d/k_{t11}k_{t22})^{1/2}[m_2]^2[m_0]^{1/2}H$$

Balance Equations

Initiator

$$-\frac{d[m_0]}{dt} = k_d[m_0]$$

Comonomers

$$-\frac{d[m_1]}{dt} = R_{p11} + R_{p12}$$

$$-\frac{d[m_2]}{dt} = R_{p12} + R_{p22}$$

$$-\frac{d[m]}{dt} = -\frac{d[m_1]}{dt} - \frac{d[m_2]}{dt}$$

Thermal Energy

$$\rho C_p \frac{dT}{dt} = \sum_i \sum_j (-\Delta H_{ij})R_{pij} - \left(\frac{U}{l}\right)(T - T_R)$$

$$= [-\Delta H_{11}k_{p11}k_{p21}[m_1]^2 - (\Delta H_{12} + \Delta H_{21})k_{p12}k_{p21}[m_1][m_2]$$

$$-\Delta H_{22}k_{p22}k_{p12}[m_2]^2]\left(\frac{fk_d}{k_{t11}k_{t22}}\right)^{1/2}[m_0]^{1/2}H - \left(\frac{U}{l}\right)(T - T_R)$$

where $l \equiv V/A_w$

In the present study we use the phi-factor model throughout. When appropriate, parallel expressions for the other models will be tabulated for completeness. While the penultimate-effect model appears to be the best one, since it alone accounts for the influence of temperature variations on cross-termination reactions, requisite data for the model parameters are scant. Only those for the systems styrene–methyl methacrylate and styrene–butyl acrylate seem to be available.[14,15]

However, in the analysis that follows, the form used is general and not tied to any one particular system. It should apply regardless of the termination mode chosen. The functional form of the parameters will accommodate to changes in mechanism, but critical values of the key parameters will remain the same.

BALANCE EQUATIONS

As in our earlier work,[1] we write material and energy balances for a well-mixed batch reactor with heat transfer to a reservoir at constant temperature T_R. All thermodynamic properties were again taken to be constant. We also applied the long-chain approximation (LCA), $R_{i1} \ll R_{p1}$, $R_{i2} \ll R_{p2}$, and $R_i \ll R_p$, to obtain the following approximations:

$$-d[\mathrm{A}]/dt = R_{i1} + R_{p1} \approx R_{p1} \tag{6}$$

Table VI

Dimensionless Termination Function

$$H' = H/(H)_o$$

Geometric Mean

$$H' = \frac{(x_1)_o(r_1)_o{}^{\lambda}{}_1 + (x_2)_o(r_2)_o{}^{\lambda}{}_2}{(x_1)_o(r_1)_o{}^{\lambda}{}_1 m_1 \exp \frac{E'_{pt21}T'}{2(1+T')} + (x_2)_o(r_2)_o{}^{\lambda}{}_2 m_2 \exp \frac{E'_{pt12}T'}{2(1+T')}}$$

Phi Factor

$$H' = \frac{((x_1)_o(r_1)_o{}^{\lambda}{}_1)^2 + 2\phi(x_1)_o(r_1)_o{}^{\lambda}{}_1(x_2)_o(r_2)_o{}^{\lambda}{}_2 + ((x_2)_o(r_2)_o{}^{\lambda}{}_2)^2}{((x_1)_o(r_1)_o{}^{\lambda}{}_1)^2 m_1^2 \exp \frac{E'_{pt21}T'}{2(1+T')} + 2\phi(x_1)_o(r_1)_o{}^{\lambda}{}_1(x_2)_o(r_2)_o{}^{\lambda}{}_2 m_1 m_2 \exp \frac{(E'_{pt12}+E'_{pt21})T'}{2(1+T')} + ((x_2)_o(r_2)_o{}^{\lambda}{}_2)^2 m_2^2 \exp \frac{E'_{pt12}T'}{2(1+T')}}$$

Penultimate Effect

$$H' = \frac{(x_1)_o(r_1)_o{}^{\lambda}{}_1 \left[\frac{(x_1)_o(r_1)_o + (x_2)_o{}^{\Delta}{}_1}{(x_1)_o(r_1)_o + (x_2)_o}\right] + (x_2)_o(r_2)_o{}^{\lambda}{}_2 \left[\frac{(x_2)_o(r_2)_o + (x_1)_o{}^{\Delta}{}_2}{(x_2)_o(r_2)_o + (x_1)_o}\right]}{(x_1)_o(r_1)_o{}^{\lambda}{}_1 m_1 \exp \frac{E'_{pt21}T'}{2(1+T')} \left[\frac{(x_1)_o(r_1)_o m_1 \exp \frac{E'_{r1}T'}{(1+T')} + (x_2)_o{}^{\Delta}{}_1 m_2 \exp \frac{E'_{D1}T'}{(1+T')}}{(x_1)_o(r_1)_o m_1 \exp \frac{E'_{r1}T'}{(1+T')} + (x_2)_o m_2}\right] + (x_2)_o(r_2)_o{}^{\lambda}{}_2 m_2 \exp \frac{E'_{pt12}T'}{2(1+T')} \left[\frac{(x_2)_o(r_2)_o m_2 \exp \frac{E'_{r2}T'}{(1+T')} + (x_1)_o{}^{\Delta}{}_2 m_1 \exp \frac{E'_{D2}T'}{(1+T')}}{(x_2)_o(r_2)_o m_2 \exp \frac{E'_{r2}T'}{(1+T')} + (x_1)_o m_1}\right]}$$

TABLE VII
Semidimensionless balances

Semidimensionless Balances

Initiator

$$-\frac{dm_0}{dt} = \left(\frac{m_0}{\lambda_i}\right)\exp\left[\frac{E'_d T'}{1+T'}\right]$$

Comonomers

$$-\frac{dm_1}{dt} = \frac{R'_{11}}{\lambda_{m11}} + \frac{R'_{12}}{\lambda_{m21}} = \left\{\frac{m_1^2 m_0^{1/2}}{\lambda_{m11}}\exp\left[\frac{E'_{11}T'}{1+T'}\right] + \frac{m_1 m_2 m_0^{1/2}}{\lambda_{m21}}\exp\left[\frac{E'_{12}T'}{1+T'}\right]\right\} H'$$

$$-\frac{dm_2}{dt} = \frac{R'_{12}}{\lambda_{m12}} + \frac{R'_{22}}{\lambda_{m22}} = \left\{\frac{m_1 m_2 m_0^{1/2}}{\lambda_{m12}}\exp\left[\frac{E'_{12}T'}{1+T'}\right] + \frac{m_2^2 m_0^{1/2}}{\lambda_{m22}}\exp\left[\frac{E'_{22}T'}{1+T'}\right]\right\} H'$$

$$-\frac{dm}{dt} = \left\{\left[\frac{(x_1)_0 m_1^2 m_0^{1/2}}{\lambda_{m11}}\right]\exp\left[\frac{E'_{11}T'}{1+T'}\right] + \left[\frac{(x_1)_0}{\lambda_{m21}} + \frac{(x_2)_0}{\lambda_{m12}}\right] m_1 m_2 m_0^{1/2}\exp\left[\frac{E'_{12}T'}{1+T'}\right] + \left[\frac{(x_2)_0 m_2^2 m_0^{1/2}}{\lambda_{m22}}\exp\left[\frac{E'_{22}T'}{1+T'}\right]\right\} H'$$

Thermal Energy Balance

$$\frac{dT'}{dt} = \left\{\left(\frac{m_1^2 m_0^{1/2}}{\lambda_{G11}}\right)\exp\left[\frac{E'_{11}T'}{1+T'}\right] + \left(\frac{1}{\lambda_{G12}} + \frac{1}{\lambda_{G21}}\right) m_1 m_2 m_0^{1/2}\exp\left[\frac{E'_{12}T'}{1+T'}\right] + \left(\frac{m_2^2 m_0^{1/2}}{\lambda_{G22}}\right)\exp\left[\frac{E'_{22}T'}{1+T'}\right]\right\} H' - \frac{T' - T'_R}{\lambda_R}$$

$$-d[\mathrm{B}]/dt = R_{i2} + R_{p2} \approx R_{p2} \tag{7}$$

$$-d[m]/dt = R_i + R_p \approx R_p \tag{8}$$

where $[m] = [\mathrm{A}] + [\mathrm{B}]$. By making use of the expressions in Tables II and IV, the balance equations listed in Table V were obtained. We point out that the effects of the termination mechanism are all lumped into function H.

By virtue of the LCA, the heat of copolymerization in the thermal energy balance was attributed entirely to the four propagation reactions. The values of ΔH_{ii} for the mutual propagation reactions were assumed to be the same as for the corresponding homopolymerizations. Concerning cross-propagation enthalpies ΔH_{ij}, data are available for their sum, $\Delta H_{12} + \Delta H_{21}$, for a number of comonomer systems.[16,17] While we have used them separately in formulating our balances for convenience of nomenclature, application of the QSSA leads to the conclusion that knowledge of their sum is sufficient to perform all computations. Thus, from the symmetry condition in Table II,

$$\Delta H_{12}R_{p12} + \Delta H_{21}R_{p21} = (\Delta H_{12} + \Delta H_{21})R_{pij} \tag{9}$$

As before,[1] we identify characteristic times (time constants) for the process by reducing all concentrations and temperatures in the balances of Table V to dimensionless form, thus rendering all equations semidimensionless (units of reciprocal time). The results are listed in Tables VI and VII. Of the two types of dimensionless temperature employed in our earlier work,[1-4] T' and $\theta \equiv E'T'$, it was necessary in the present study to use the former since there is no a priori criterion for choosing an appropriate dimensionless activation energy E' for copolymerization from among the four alternatives available. We note that a change in termination mode does not affect the general form of the balances. Function H is a factorable term common to all dimensionless rate expressions and contains all parameters specific to a particular mechanism.

TABLE VIII
Lumped Characteristic Times

$$\Lambda_1 \equiv \left(\frac{1}{\lambda_{m11}} + \frac{1}{\lambda_{m21}}\right)^{-1} = \left(\frac{(r_1)_0(x_1)_0 + (x_2)_0}{(r_1)_0\lambda_1(r_2)_0\lambda_2[m]_0\sqrt{R_{i0}}/(H)_0}\right)^{-1}$$

$$\Lambda_2 \equiv \left(\frac{1}{\lambda_{m22}} + \frac{1}{\lambda_{m12}}\right)^{-1} = \left(\frac{(r_2)_0(x_2)_0 + (x_1)_0}{[(r_1)_0\lambda_1(r_2)_0\lambda_2[m]_0\sqrt{R_{i0}}/(H)_0}\right)^{-1}$$

$$\Lambda_m \equiv \left[\frac{(x_1)_0}{\lambda_{m11}} + \frac{(x_2)_0}{\lambda_{m12}} + \frac{(x_1)_0}{\lambda_{m21}} + \frac{(x_2)_0}{\lambda_{m22}}\right]^{-1} = \left[\frac{(r_1)_0(x_1)_0^2 + 2(x_1)_0(x_2)_0 + (r_2)_0(x_2)_0^2}{(r_1)_0\lambda_1(r_2)_0\lambda_2[m]_0\sqrt{R_{i0}}/(H)_0}\right]^{-1}$$

$$\Lambda_G \equiv \left[\frac{1}{\lambda_{G11}} + \frac{1}{\lambda_{G12}} + \frac{1}{\lambda_{G21}} + \frac{1}{\lambda_{G22}}\right]^{-1}$$

$$= \left[\frac{(r_1)_0(x_1)_0He_{11} + (x_1)_0He_{12} + (x_2)_0He_{21} + (r_2)_0(x_2)_0He_{22}}{(r_1)_0\lambda_1(r_2)_0\lambda_2[m]_0\sqrt{R_{i0}}/(H)_0}\right]^{-1}$$

$$\Lambda_{ad} \equiv \left[\left(\frac{E'_{11}}{\lambda_{G11}} + \frac{E'_{12}}{\lambda_{G12}} + \frac{E'_{12}}{\lambda_{G21}} + \frac{E'_{22}}{\lambda_{G22}}\right) + \frac{\partial H'}{\partial T'}\Big/\Lambda_G\right]^{-1}$$

$$= \left[\left((r_1)_0(x_1)He_{11}\left(E'_{11} + \frac{\partial H'}{\partial T'}\right) + (x_2)_0He_{12}\left(E'_{12} + \frac{\partial H'}{\partial T'}\right) + (x_1)_0He_{21}\left(E'_{12} + \frac{\partial H'}{\partial T'}\right)\right.\right.$$

$$\left.\left. + (r_2)_0(x_2)_0He_{22}\left(E'_{22} + \frac{\partial H'}{\partial T'}\right)\right)\Big/(r_1)_0\lambda_1(r_2)_0\lambda_2[m]_0\sqrt{R_{i0}}/(H)_0\right]^{-1}$$

TABLE IX
Characteristic Times and Dimensionless Groups not Defined in Text

$$\lambda_i = (R_{i0}/f(m_0)_0)^{-1} = 1/(k_d)_0$$

$$\lambda_R = \rho C_p/(U/l)$$

$$\lambda_j = (k_{pjj0}\sqrt{R_{i0}/k_{tjj0}})^{-1} \qquad j = 1, 2$$

$$\lambda_{mij} = [(R_{pij})_0/[m_j]_0]^{-1} \qquad i = 1, 2 \qquad j = 1, 2$$

$$He_{ij} = (-\Delta H_{ij})[m_j]_0/\rho C_p T_0 \qquad i = 1, 2 \qquad j = 1, 2$$

$$\lambda_{Gij} = \lambda_{mij}/He_{ij} \qquad i = 1, 2 \qquad j = 1, 2$$

$$\Delta_j = k_{tijji}/k_{tjjjj} \qquad i = 1, 2 \qquad j = 1, 2 \qquad i \neq j$$

$$E'_{Dj} = (E_{tijji} - E_{tjjjj})/RT_0 \qquad i = 1, 2 \qquad j = 1, 2 \qquad i \neq j$$

$$E'_{jk} = \left(E_{pjl} - E_{plj} + \frac{1}{2}(E_d - E_{tjj} - E_{tll})\right)\Big/ RT_0 \qquad \begin{matrix} j \neq l = 1, 2 \\ j = 1, 2 \end{matrix}$$

$$E'_{ptij} = (2E_{pij} - E_{tii})/RT_0 \qquad i = 1, 2 \qquad j = 1, 2$$

$$\gamma_{Tij} = \lambda_{Gij}/\lambda_R$$

TABLE X
Kinetic Constants and Physical Data

Comonomers	r_1	r_2	φ	$-(\Delta H_{12} + \Delta H_{21})$, kcal
S/AN	$2.56 \exp(-599/T)$	$6.67 \times 10^{-5} \exp(2184/T)$	23	34.7
S/MMA	$1.83 \exp(-450/T)$	$1.27 \exp(-340/T)$	13	31.7
AN/MMA	$0.59 \exp(260/T)$	$1.94 \exp(-916/T)$	200	28.4

Monomer	k_p, l./mole-sec	k_t, l./mole-sec	$[m]_0$, mole/l.	ρ, g/cc	C_p, cal/g	$-\Delta H$, kcal
S	$1.057 \times 10^7 \exp(-3557/T)$	$1.255 \times 10^9 \exp(-843/T)$	8.7	0.91	0.4	16.7
MMA	$9 \times 10^5 \exp(-2365/T)$	$1.1 \times 10^8 \exp(-604/T)$	9.5	0.95	0.3	13.5
AN	$3 \times 10^7 \exp(-2063/T)$	$3.3 \times 10^{12} \exp(-2718/T)$	15.2	0.81	0.4	18.4

Initiator	k_d, sec^{-1}
BP	$2 \times 10^{13} \exp(-15098/T)$
AIBN	$10^{15} \exp(-15350/T)$
DTBP	$4.3 \times 10^{15} \exp(-18620/T)$

If we employ a shorthand notation here, it is possible to write the thermal energy balance for copolymerization as in Table VII:

$$\frac{dT'}{dt} = \sum_{i=1}^{2}\sum_{j=1}^{2}(R'_{ij}/\lambda_{Gij}) - [(T' - T'_R)/\lambda_R] \tag{10}$$

$$\equiv G_e(T',t) - R_e(T') \tag{11}$$

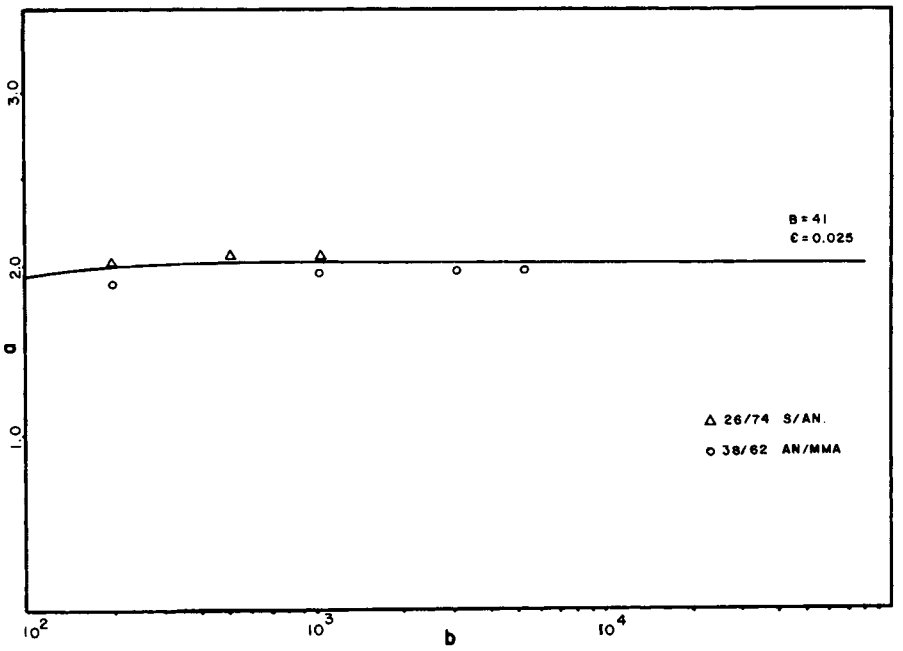

Fig. 1. Dimensionless runaway boundary a_{cr} vs. b.

similar to that for homopolymerization[1]:

$$\frac{dT'}{dt} = (R'/\lambda_G) - (T' - T'_R)/\lambda_R \tag{12}$$

$$\equiv G_e(T',t) - R_e(T') \tag{13}$$

where the dimensionless rate function R'_{ij} is again written in a form

$$R'_{ij} = R'_{ij}(T',t) \equiv F_{ij}(t)g_{ij}(T')H'(T',t) \tag{14}$$

$$F_{ij}(t) \equiv m_i m_j m_0^{1/2} \tag{15}$$

This facilitates the separation of a dimensionless temperature-dependent generation function

$$g_{ij}(T') \equiv \exp\,[E'_{ij}T'/(1 + T')] \tag{16}$$

but does not permit removal of the explicit temperature dependence from the remaining dimensionless concentration portion of G_e, viz., $F_{ij}(t)H'(T',t)$, as before,[1] owing to the presence of function H.

Both m_i and $H'(T,t)$ arise from the dimensionless expressions for the active intermediates. In homopolymerization, the concentration of intermediates could be expressed solely in terms of initiator concentration and temperature. The intermediate concentrations in copolymerization are also functions of these factors, and in addition they are dependent upon the composition of the comonomers. As may be noted in the tables, $H'(T,t)$ is a function of the comonomer concentrations and must therefore change with time. However, the product of

TABLE XI
Simulation Results

Case	System	x_1	T_0, °K	$[I]_0$, mole/l.	U/l, cal/cc sec °K	B	E'	b	a	RA
1	S/AN/BP	0.5	398	0.163	8.97×10^{-2}	35.2	25.7	195	1.97	no
2					8.92				1.96	yes
3		0.6	383	0.0763	2.04×10^{-2}	35.8	26.8	195	1.96	no
4					2.03				1.95	yes
5		0.7	373	0.0517	7.07×10^{-3}	35.6	27.6	195	1.935	no
6					7.05				1.93	yes
7		0.8	363	0.0358	2.32×10^{-3}	35.6	28.6	195	1.918	no
8					2.29				1.90	yes
9	AN/MMA/BP	0.2	322	1.33×10^{-4}	1.57×10^{-5}	45	28.6	300	2.025	no
10					1.55				1.998	yes
11		0.4	336	8.33×10^{-4}	1.03×10^{-4}	45	26.5	300	1.986	no
12					1.02				1.976	yes
13		0.6	353	7.75×10^{-3}	1.01×10^{-3}	45	24.8	300	1.975	no
14					0.96				1.96	yes
15		0.8	378	0.119	1.61×10^{-2}	45	23.5	300	1.998	no
16					1.60				1.985	yes
17	S/MMA/BP	0.2	318	1.21×10^{-3}	8.99×10^{-6}	45	31.3	300	2.075	no
18					8.88				2.05	yes
19		0.4	314	9.76×10^{-4}	4.81×10^{-6}	45	31.8	300	2.075	no
20					4.75				2.05	yes
21		0.6	309	7.27×10^{-4}	2.42×10^{-6}	45	32.6	300	2.075	no
22					2.39				2.05	yes
23		0.8	306	7.44×10^{-4}	1.54×10^{-6}	45	33.5	300	2.05	no
24					1.52				2.026	yes
25	S/AN/DTBP	0.7	403	0.05	1.04×10^{-2}	36	30	400	1.985	no
26					1.03				1.975	yes

(TABLE XI con't)

27	S/AN/BP		373	0.07	8.28×10^{-3}	35.6	27.6	229	1.95	no
28					8.24				1.94	yes
29				0.025	4.86×10^{-3}			136	1.915	no
30					4.82				1.90	yes
31				0.01	3.01×10^{-3}			86	1.875	no
32					2.97				1.85	yes
33	S/AN/AIBN			0.10	3.55×10^{-2}	36.0	28.0	42	1.77	no
34					3.49				1.74	yes
35				0.05	2.37×10^{-2}			30	1.67	no
36					2.34				1.65	yes

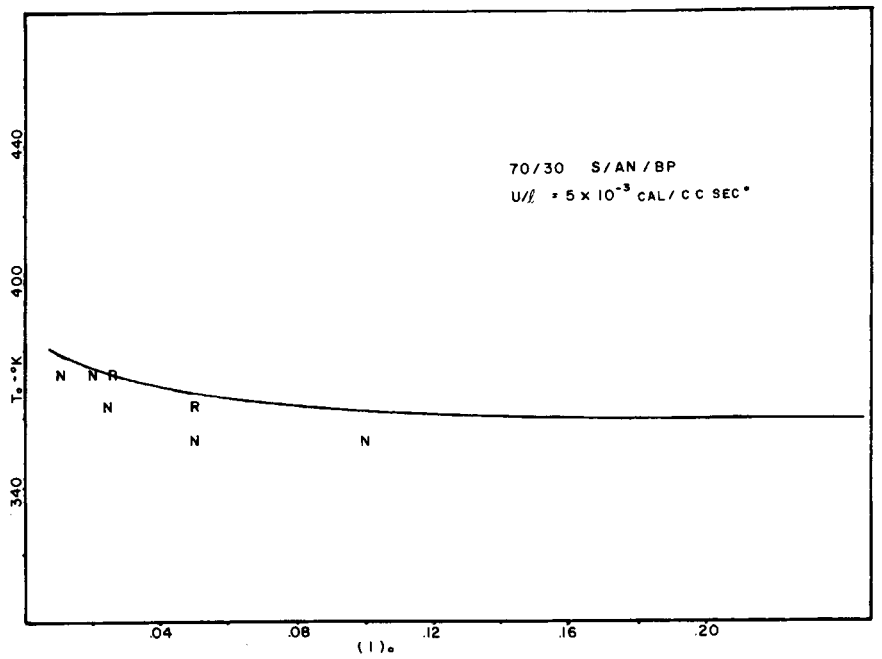

Fig. 2. Predicted runaway boundary with experimental points.

m_i and $H'(T',t)$ is a function of concentration ratios. If composition drift in the monomer pool is small, then the product of $H'(T,t)$ with m_i will become a function of temperature only. For the special case of azeotropic copolymerization, where comonomer compositions remain fixed with conversion, $m_iH'(T',t)$ becomes a function of dimensionless temperature alone.

IGNITION ANALYSIS

In our ignition studies of homopolymerizations,[1] an ignition criterion was developed via a Semenov-type analysis. To accomplish this, λ_R was chosen to define dimensionless time, $\tau \equiv t/\lambda_R$, which was then used to make the energy balance completely dimensionless for subsequent mathematical manipulation. The presence of the additional function H does not, per se, preclude the use of a Semenov-type analysis here. Rather, it is the complex mathematical form of the resulting energy balance.

Following our homopolymerization analysis, we use λ_R to make our copolymer energy balance completely dimensionless:

$$\frac{dT'}{d\tau} = \sum_{i=1}^{2}\sum_{j=1}^{2} f_{ij}(\tau)g_{ij}(T')H'(T',\tau) - r_e(T') \tag{17}$$

where

$$f_{ij}(\tau) \equiv F_{ij}(\tau)/\gamma_{Tij} \tag{18}$$

and

$$r_e(T') \equiv T' - T'_R \tag{19}$$

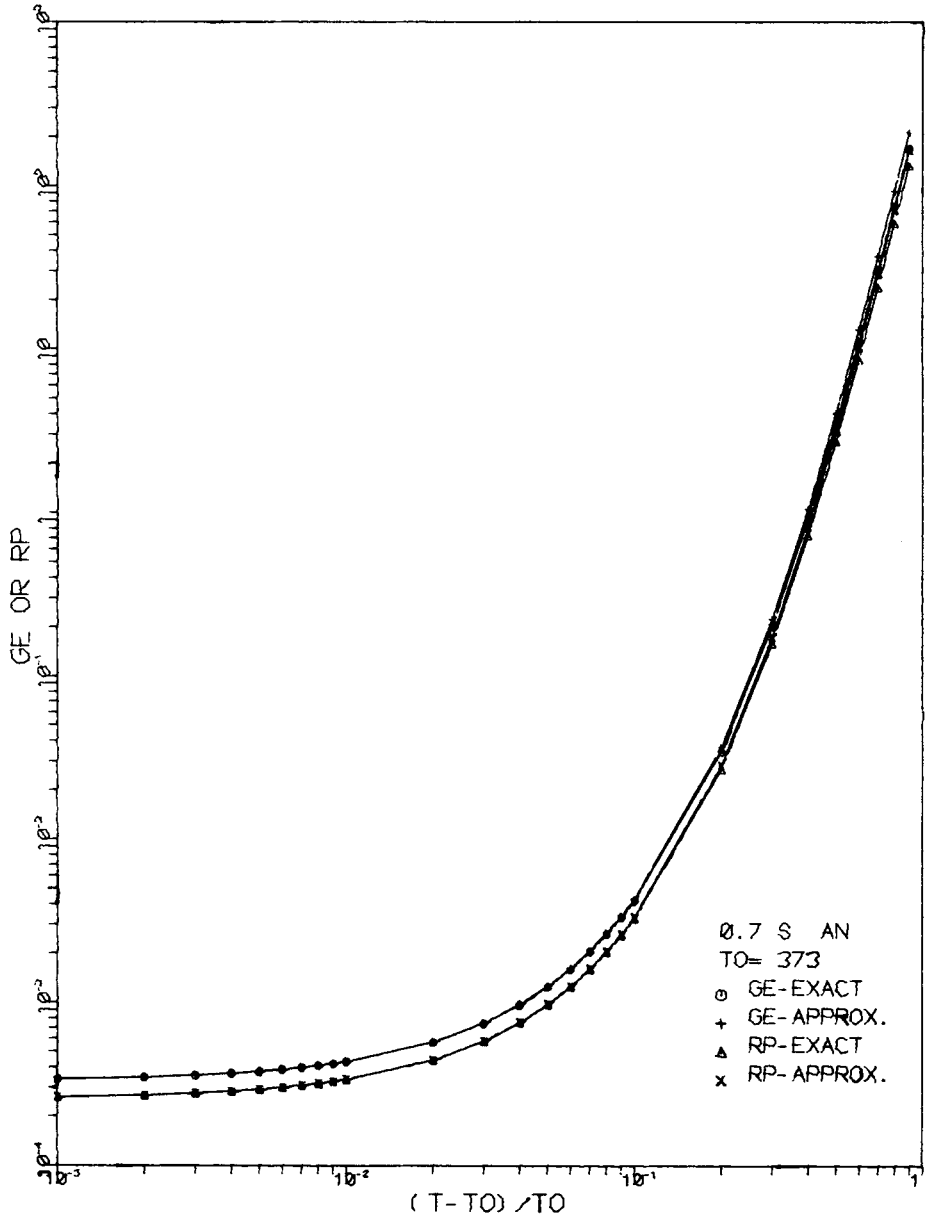

Fig. 3. Comparison of exact and approximate forms with ERA—S/AN/BP

By the early runaway approximation (ERA), we set all concentrations to their feed values with the result that

$$f_{ij} = (\gamma_{Tij})^{-1} \qquad \text{and} \qquad H'(T',\tau) = H'(T')$$

and thus the total heat generation function becomes a function of temperature only

$$\sum_{i=1}^{2}\sum_{j=1}^{2} g_{ij}(T')H'(T')/\gamma_{Tij} \equiv g_e(T') \tag{20}$$

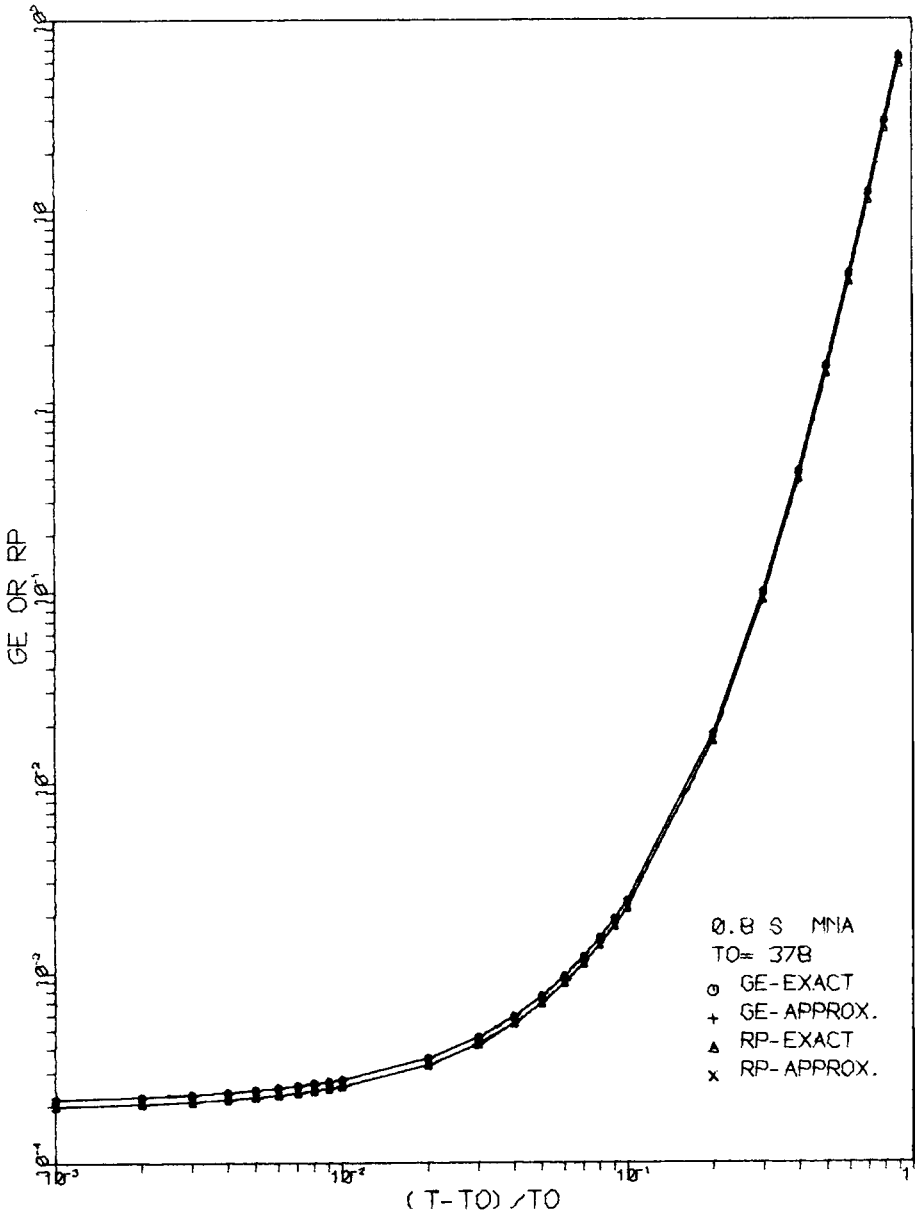

Fig. 4. Comparison of exact and approximate forms with ERA—S/MMA/BP

as before.[1] The IG temperature is then defined as the temperature which satisfies the tangency conditions $g_e(T') = r_e(T')$ and $dg_e/dT' = dr_e/dT'$. While the ensuing equations for homopolymerizations

$$\gamma_T^{-1} \exp [E'T'/(1 + T')] = T' - T'_R \tag{21}$$

$$\gamma_T^{-1}(1 + T')^{-2}E' \exp [E'T'/(1 + T')] = 1 \tag{22}$$

are analytically tractable, their counterparts for copolymerizations

$$\sum_{i=1}^{2} \sum_{j=1}^{2} \gamma_{Tij}^{-1} \{\exp [E_{ij}T'/(1 + T')\} H'(T') = T' - T'_R \tag{23}$$

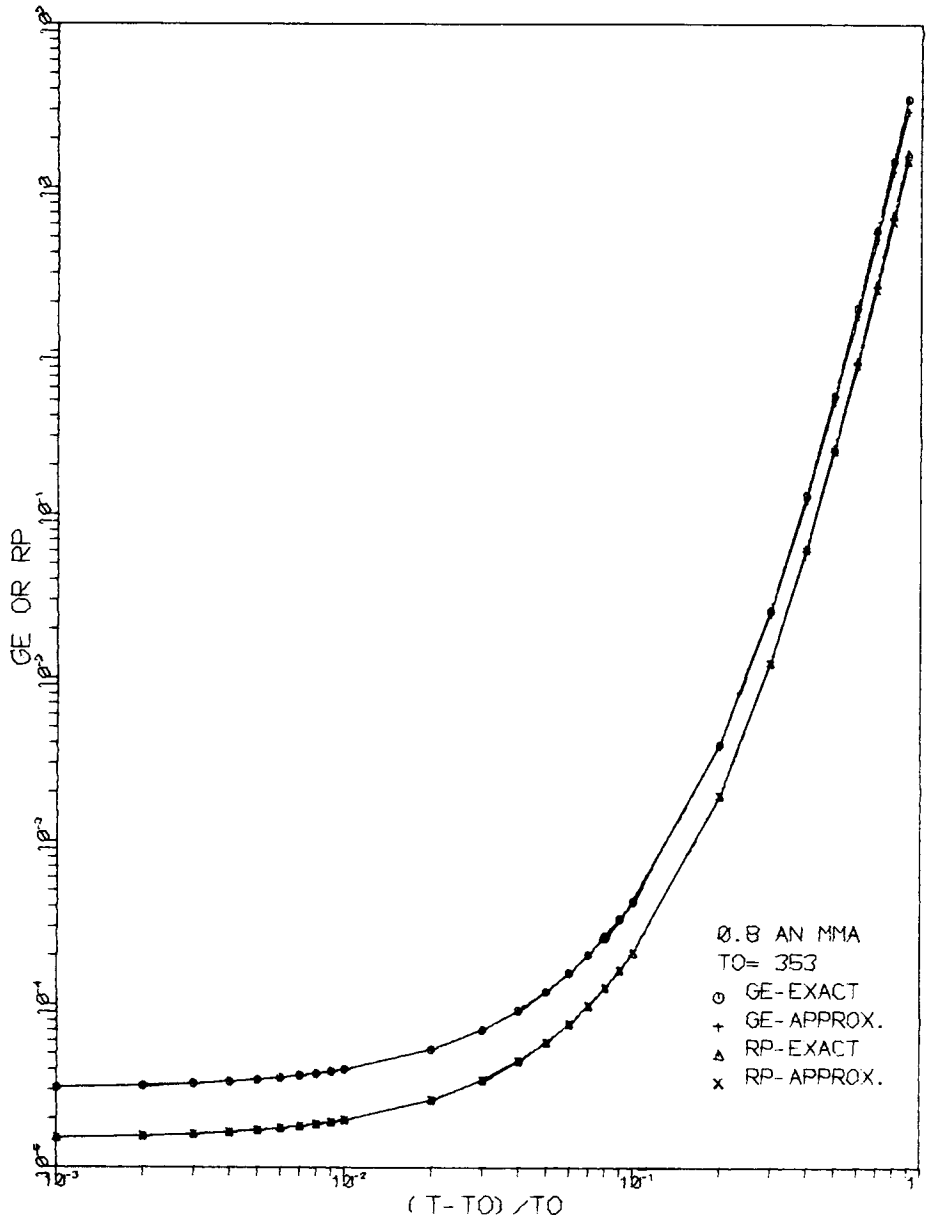

Fig. 5. Comparison of exact and approximate forms with ERA—AN/MMA/DTBP

$$\sum_{i=1}^{2}\sum_{j=1}^{2}\left\{\left(\gamma_{Tij}^{-1}(1+T')^{-2}E'_{ij}H'(T')+\gamma_{Tij}^{-1}\frac{dH'}{dT'}\right)\exp\left[E'_{ij}T'/(1+T')\right\}\right\}=1 \quad (24)$$

are not, owing to the sum of exponentials in temperature, each with a different activation energy, multiplied by functions of temperature H' and dH'/dT'. An alternate approach is clearly required.

What we seek is a set of appropriate dimensionless parameters, such as a, B, and b, together with relationships in terms of them, such as inequalities (1), (2), and (3), which characterize the thermal behavior of copolymerizations. Our

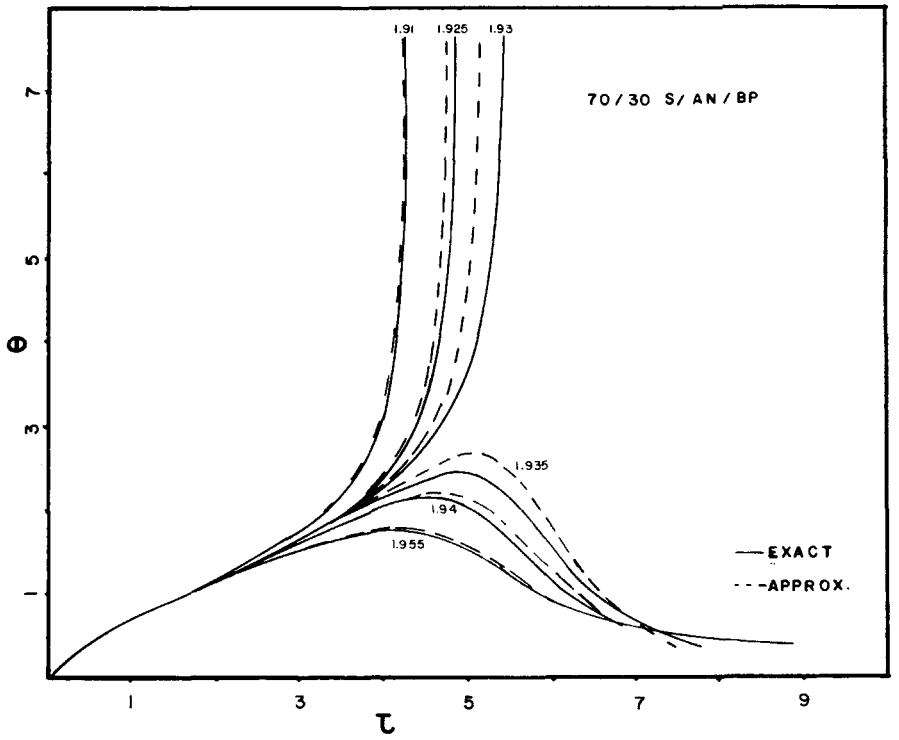

Fig. 6. Exact and approximate transition temperature profiles for near azeotropic system.

technique has been to begin with characteristic times and evolve dimensionless groups in terms of these which have intuitive physical meaning. We begin here by reexamining our previous definitions of characteristic times. The dimensionless rate function for homopolymerization was[2,3]

$$R' = mm_0^{1/2} \exp\left[E'T'/(1 + T')\right] \tag{25}$$

and the semidimensionless monomer energy balance was,[2,3] with the LCA,

$$-dm/dt = R'/\lambda_m \tag{26}$$

Since under feed conditions $R' = (R')_0 = 1$, it is clear from eq. (26) that λ_m^{-1} may be interpreted as the initial polymerization rate

$$\lambda_m^{-1} = (-dm/dt)_0 \tag{27}$$

This is a somewhat different meaning than the one attached to λ_m based upon its original definition.[2] Similarly, from eq. (13) we obtain

$$\lambda_G^{-1} = (G_e)_0 \tag{28}$$

which indicates that λ_G^{-1} is the initial heat generation rate.

We now extend this line of analysis to copolymerizations. Thus, from the total monomer balance in shorthand notation

$$-\frac{dm}{dt} = \sum_{i=1}^{2} \sum_{j=1}^{2} \frac{(x_j)_0 R'_{ij}}{\lambda_{mij}} \tag{29}$$

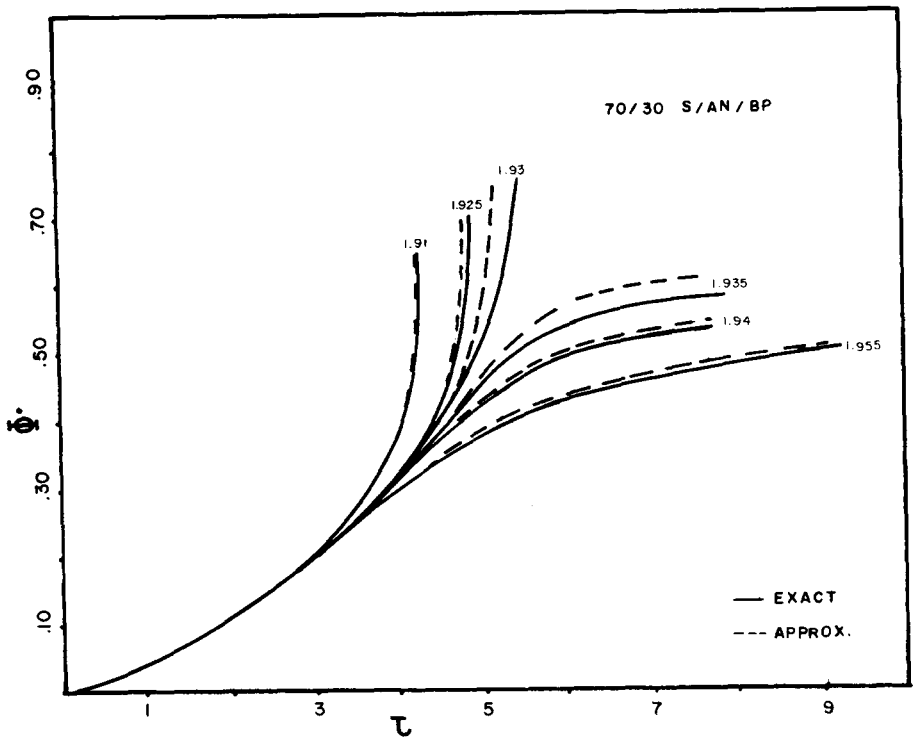

Fig. 7. Exact and approximate transition conversion profiles for near azeotropic system.

we obtain a lumped-parameter version of the characteristic time for monomer conversion Λ_m, which may be interpreted as the reciprocal of the initial copolymerization rate

$$\left(\frac{dm}{dt}\right)_0 = \frac{(x_1)_0}{\lambda_{m11}} + \frac{(x_2)_0}{\lambda_{m12}} + \frac{(x_1)_0}{\lambda_{m21}} + \frac{(x_2)_0}{\lambda_{m22}} \equiv \Lambda_m^{-1} \tag{30}$$

Similarly, for individual comonomers we obtain

$$\left(-\frac{dm_1}{dt}\right)_0 = \left(\frac{1}{\lambda_{m11}} + \frac{1}{\lambda_{m21}}\right) \equiv \Lambda_1^{-1} \tag{31}$$

$$\left(-\frac{dm_2}{dt}\right)_0 = \left(\frac{1}{\lambda_{m12}} + \frac{1}{\lambda_{m22}}\right) \equiv \Lambda_2^{-1} \tag{32}$$

with the relationship among them

$$\Lambda_m^{-1} = (x_1)_0\Lambda_1^{-1} + (x_2)_0\Lambda_2^{-1} \tag{33}$$

and from the thermal energy balance, applying eq. (28),

$$(G_e)_0 = \frac{1}{\lambda_{G11}} + \frac{1}{\lambda_{G12}} + \frac{1}{\lambda_{G21}} + \frac{1}{\lambda_{G22}} \equiv \Lambda_G^{-1} \tag{34}$$

Concerning the latter, however, it should be pointed out that the key parameter in characterizing R-A in homopolymerizations was

$$a \equiv \lambda_{ad}/\lambda_R \tag{35}$$

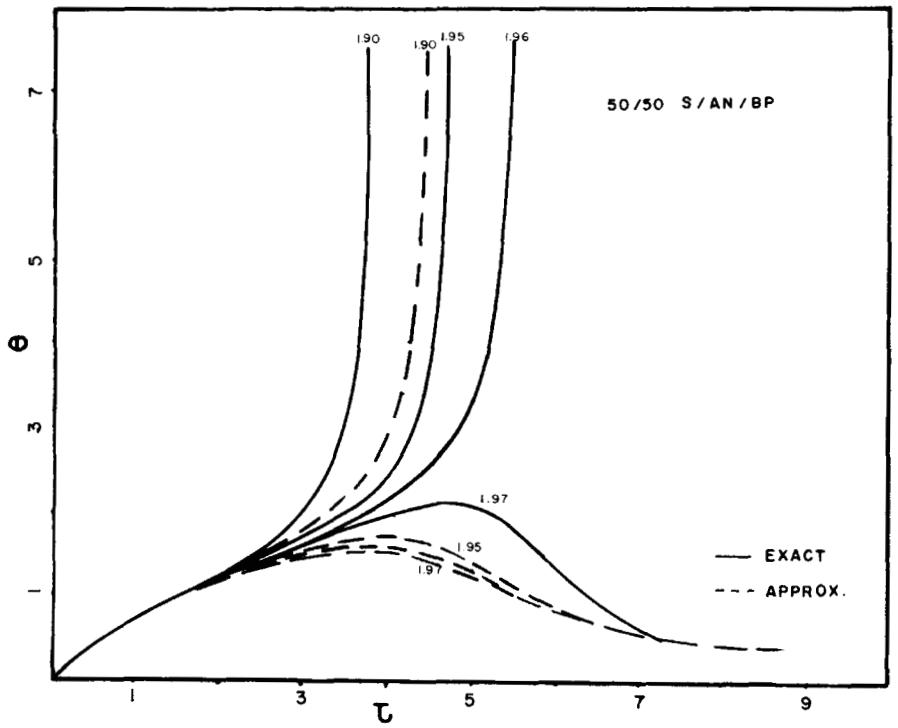

Fig. 8. Exact and approximate transition temperature profiles for "hotter" approximate form.

which contained λ_{ad}

$$\lambda_{ad} \equiv \lambda_G/E' \tag{36}$$

as opposed to λ_G. We recall that λ_{ad} was contained in the first term (R'/λ_{ad}) of the counterpart of eq. (12), obtained by using $\theta \equiv E'T'$ as the dimensionless temperature in transforming the thermal energy balance to semidimensionless form. Clearly, we cannot define the copolymer version of λ_{ad}, viz., Λ_{ad}, simply by applying eq. (36) to the definition of Λ_G, eq. (34), because, as previously pointed out, no single activation energy or combination of activation energies for copolymerization suggests itself as an appropriate substitute for E'. Furthermore, λ_R in definition (35) is not simply equal to $(R_e)_0$. Consequently, a modification of this approach is required.

We observe from the energy balance for homopolymerizations, obtained by substituting eq. (25) into (12), that the required characteristic times λ_{ad} and λ_R may be identified in a systematic and consistent fashion as follows:

$$(\partial G_e/\partial T')_0 = E'/\lambda_G \equiv 1/\lambda_{ad} \tag{37}$$

$$(\partial R_e/\partial T')_0 = 1/\lambda_R \tag{38}$$

so that

$$a = \frac{(\partial R_e/\partial T')_0}{(\partial G_e/\partial T')_0} \tag{39}$$

This characterizes R-A as a competition between the degree to which heat gen-

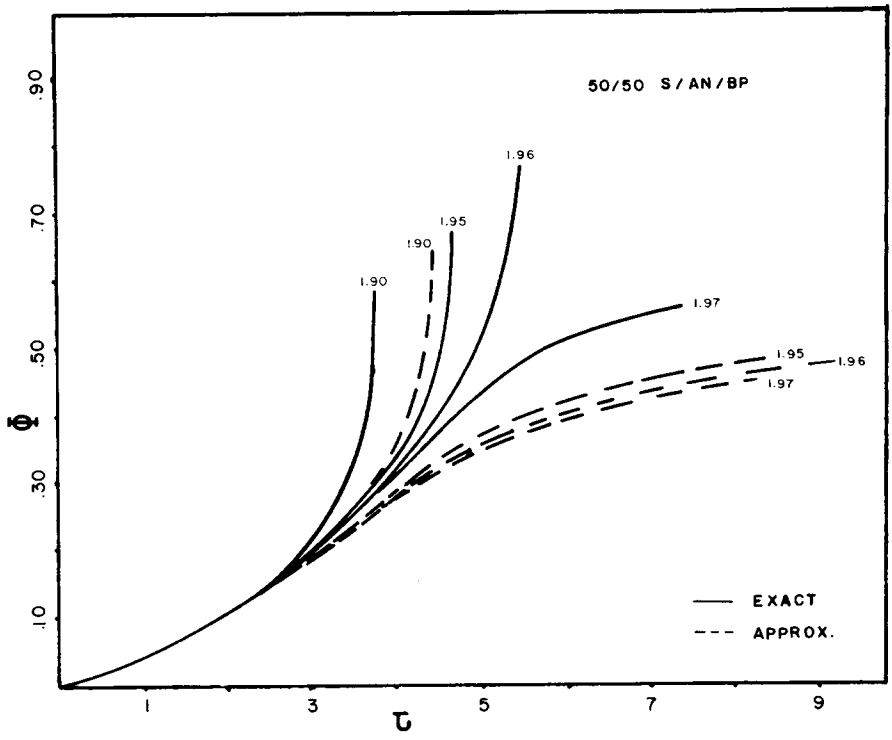

Fig. 9. Exact and approximate transition conversion profile for "hotter" approximate form.

eration rate rises with temperature and the degree to which heat removal rate can match that rise.

Applying definition (37) to copolymerizations for which $\partial G_e/\partial T'$ is

$$\frac{\partial G_e}{\partial T'} = \sum\sum [H(T')E'_{ij}/\lambda_{Gij}(1 + T')^2] \exp [E'_{ij}T'/(1 + T')] + \sum\sum [(1/\lambda_{Gij}) \exp E'_{ij}T'/(1 + T')] \frac{\partial H'}{\partial T'} \quad (40)$$

yields, when evaluated under feed conditions where $T' = 0$ and $H' = 1$,

$$\left(\frac{\partial G_e}{\partial T'}\right)_0 = \sum_{i=1}^{2}\sum_{j=1}^{2} \left(\frac{E'_{ij}}{\lambda_{Gij}}\right) + \left(\frac{\partial H'}{\partial T'}\right)_0 \Lambda_G^{-1} \equiv \Lambda_{ad}^{-1} \quad (41)$$

Thus, we propose that the R-A criterion for copolymerizations is inequality (1) with

$$a \equiv \Lambda_{ad}/\lambda_R \quad (42)$$

Having now defined a copolymer counterpart to R-A parameter a, we proceed in a similar manner to define counterparts to parameters B and b in inequalities (2) and (3) which characterize R-A sensitivity (instability) as well as degree of reliability of the ERA:

$$B \equiv \Lambda_m/\Lambda_{ad} \quad (43)$$

$$b \equiv \lambda_i/\Lambda_{ad} \quad (44)$$

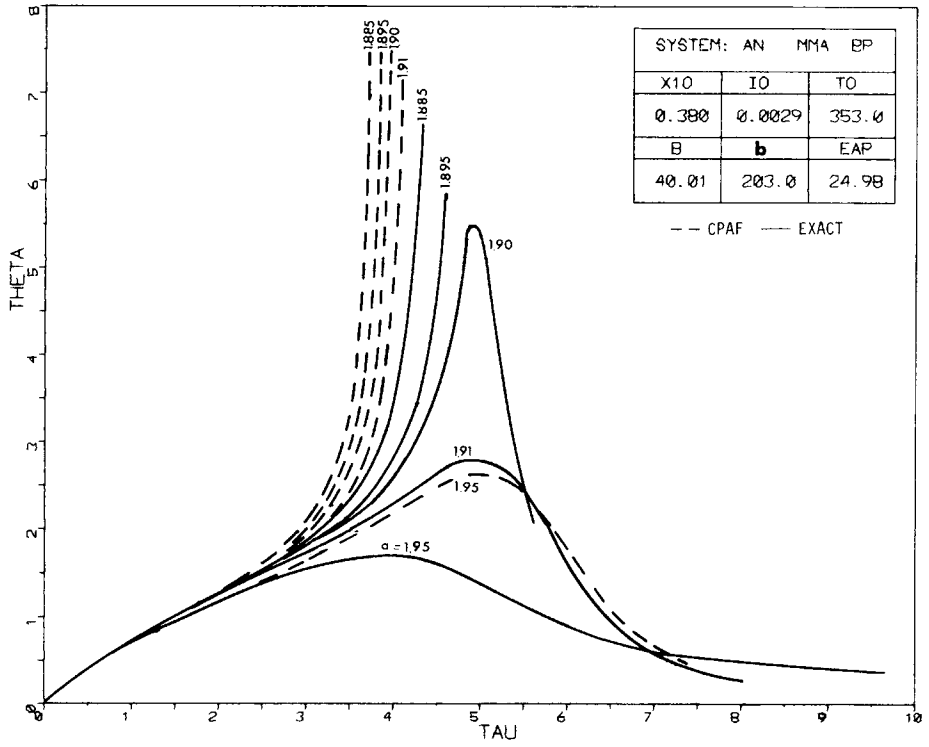

Fig. 10. Exact and approximate transition temperature profile for "cooler" approximate form.

Characteristic times and dimensionless parameters for copolymerizations are summarized in Tables VIII and IX.

AN APPROXIMATE KINETIC MODEL

As discussed in the results section that follows, numerous computer simulations as well as experiments have confirmed that the proposed criteria do indeed characterize thermal R-A of copolymerizations. We therefore extend our analysis of the apparent symmetry of form between homopolymerization and copolymerization kinetics in an effort to simplify the complex kinetic models for copolymerization. Thus, following the form of the rate function, monomer balance and thermal energy balance for homopolymerization, eqs. (25), (26), and (12), respectively, we propose the following approximate equations for copolymerizations in place of the corresponding ones in Table VII:

$$-dm/dt = R'/\Lambda_m \tag{45}$$

and

$$dT'/dt = R'/\Lambda_G - (T' - T'_R)/\lambda_R \tag{46}$$

where

$$R' \equiv mm_0^{1/2} \exp\,[E'T'/(1 + T')] \tag{47}$$

and

$$E' \equiv \Lambda_G/\Lambda_{ad} \tag{48}$$

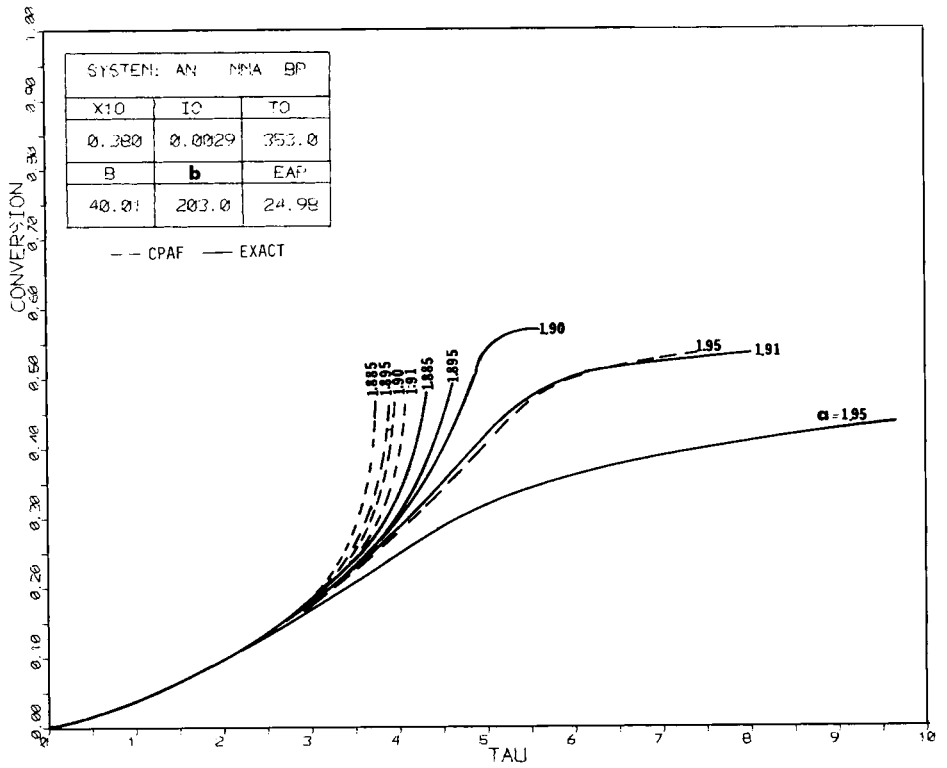

Fig. 11. Exact and approximate transition conversion profile for "cooler" approximate form.

It is important to point out that definition (48) follows its homopolymer counterpart, which is (reference 3, Table VII)

$$E'_{ap} = \lambda_G/\lambda_{ad} \equiv 1/\epsilon \tag{49}$$

These approximate forms for the balance equations are reasonable and should certainly be valid during early stages of nonisothermal copolymerizations since they are identical to the exact balance equations under initial conditions. Furthermore, application of the ERA to approximate eqs. (45)–(47) yields the following:

$$-\frac{dm}{dt} \approx \left(\frac{1}{\Lambda_m}\right) \exp\left[\frac{E'T'}{1+T'}\right] \tag{50}$$

$$\frac{dT'}{dt} \approx (1/\Lambda_G) \exp\left[\frac{E'T'}{1+T'}\right] - \frac{(T' - T'_R)}{\lambda_R} \tag{51}$$

which are identical to their homopolymer counterparts used in developing our R-A/IG criteria, eqs. (1)–(3), whose ability to characterize the thermal characteristics of copolymerizations has already been alluded to above. For comparison, the exact balances for copolymerization with the ERA are, from Table VII,

$$-\frac{dm}{dt} \approx \sum\sum\left[\frac{(x_j)_0}{\lambda_{mij}}\right] \exp\left[\frac{E'_{ij}T'}{1+T'}\right] H'(0,T') \tag{52}$$

$$\frac{dT'}{dt} \approx \sum\sum\left(\frac{1}{\lambda_{Gij}}\right) \exp\left[\frac{E'_{ij}T'}{1+T'}\right] H'(0,T') - \frac{(T' - T'_R)}{\lambda_R} \tag{53}$$

RESULTS

The balance equations in Table VII were solved using a Runge-Kutta numerical integration technique with variable step-size control. Reaction parameters used correspond to various combinations of styrene (S), acrylonitrite (AN), and methyl methacrylate (MMA) comonomer as listed in Table X. The results, also shown in Table XI, confirm the success of parameter a in predicting R-A behavior for a variety of systems. R-A occurs for values in the vicinity of $a = 2$, just as with homopolymerizations. Recall that Semenov analysis predicts a critical value of $a = e = 2.72$.[1] Simulation studies of homopolymerizations showed that this value decreased as the consumption of either reactant became a significant factor during the prerunaway (induction) period.[3] While either monomer or initiator depletion, or both, may cause the critical value of a to decrease, studies involving typical homopolymerization conditions show that initiator depletion is far more important in depressing the R-A boundary. Parameter b was found to characterize R-A sensitivity (IG) due to initiator depletion being rate limiting. Results in Table XI show that the critical value of a decreases as b decreases in the same manner as with homopolymerizations. We note that B, which characterizes monomer-limited IG, takes on the same range of values as it did for homopolymerization.

Previous work showed in detail the changes in the runaway boundaries caused by various dimensionless parameters.[3] Of particular interest were the boundaries of a_{cr} versus b with B as the parameter. In the present study we chose two copolymer systems with dimensionless parameters that match those in Figure 18 of reference 3. Simulation results for the 26/74 S/AN and 38/62 AN/MMA system were used to generate the boundaries which are shown in Figure 1 along with the homopolymer boundary for $B = 41$. There is close agreement between the two copolymer boundaries and the homopolymer boundary. The deviations are caused by composition drift during the inducation period.

The dimensionless criterion $a = 2$ can be numerically solved to yield T_0 versus $[I]_0$ boundaries for specific comonomer–initiator system with known heat transfer characteristics. Figure 2 shows such a boundary for benzoyl peroxide-initiated 70/30 S/AN copolymerization. The value of the heat transfer coefficient is typical of our thermal ignition point apparatus.[4] Some preliminary experimental data points (N and R) for this system are included in the figure. It should be noted that these dimensional boundaries are sensitive to the choice of kinetic mechanism used to describe the copolymerization.

The strength of our copolymerization parameter groupings in characterizing runaway in a manner paralleling homopolymerizations must be tied to the ability of approximate forms (50) and (51) to describe eqs. (52) and (53). We evaluated the approximate and exact forms of both the rate of heat generation and rate of polymerization (after application of ERA). Figures 3–5 show that the approximations track the exact forms over six decades of change in rate, and over temperature variations of nearly 100% from the feed value.

The most severe test is to compare in detail the temperature and conversion histories resulting from integrating the exact, Table VII, and approximate, eqs. (45) and (46), balances. We have done this for many systems and found the agreement to be highly variable. In all cases, the histories superimpose through roughly 20% conversion. Systems with small composition drift show close agreement for the complete reaction. Figures 6 and 7 show the transition from

runaway to nonrunaway for 70/30 S/AN/BP, a composition near the azeotrope. Even in this region of extreme sensitivity, the approximate equations reproduce the reaction profiles. Figures 8–11 illustrate the effect of substantial composition drift. The approximate profiles may be "hotter," that is, they run away at less severe conditions than the exact ones, Figures 8 and 9, or they may be "cooler," as in Figures 10 and 11. It should be noted that as the polymerization moves from the critical point toward either adiabatic or isothermal behavior, the agreement between approximate and exact profiles improves.

This work was supported in part by a grant from the National Science Foundation (ENG-7605053).

List of Symbols

a	dimensionless runaway parameter, see eqs. (35) and (42)
A_w	wetted area
[A]	concentration of monomer 1
[B]	concentration of monomer 2, see eq. (43)
B	dimensionless monomer sensitivity parameter, see eq. (44)
b	dimensionless initiator sensitivity parameter
E	activation energy
F, f	concentration forcing function, see eqs. (15) and (18)
G_e, g_e	effective generation function
g	explicitly temperature dependent generation function, see eq. (16)
ΔH	enthalpy of reaction
H	termination function defined in Table IV
$[I]$	initiator concentration
k	rate constant
m_0	dimensionless initiator concentration $[m_0]/[m_0]_0$, where $[m_0] = 2[I]$
m	dimensionless monomer concentration $[m]/[m]_0$
R	reaction rate function
R_e, r_e	effective heat removal function, see eq. (19)
T	temperature
T_r	reservoir temperature
t	time
V	volume

Greek Symbols

γ_T	λ_G/λ_R
Δ	penultimate termination ratio defined in Table IX
λ	characteristic time
Λ	lumped overall characteristic time
φ	phi-factor for cross termination, see eq. (5)

Subscripts

ad	adiabatic
G	heat generation
i	initiation (when not a numerical index)
0	initial condition
p	propagation

R heat removal
t termination

Superscripts
dimensionless quantity

References

1. J. A. Biesenberger, R. Capinpin, and D. Sebastian, *J. Appl. Polym. Sci., Appl. Polym. Symp.*, **26,** 211 (1975).
2. J. A. Biesenberger and R. Capinpin, *Polym. Eng. Sci.*, **14,** 737 (1974).
3. J. A. Biesenberger, R. Capinpin, and J. C. Yang, *Polym. Eng. Sci.*, **16,** 101 (1976).
4. D. H. Sebastian and J. A. Biesenberger, *Polym. Eng. Sci.*, **16,** 117 (1976).
5. D. H. Sebastian and J. A. Biesenberger, *J. Macromol. Sci-Chem*, submitted.
6. D. H. Sebastian and J. A. Biesenberger, *Polym. Eng. Sci.*, to appear.
7. H. W. Melville, B. Noble, and W. F. Watson, *J. Polym. Sci.*, **2,** 229 (1947).
8. P. J. Flory, *Principles of Polymer Chemistry*, Cornell University Press, Ithaca, N.Y., 1953, p. 200.
9. C. Walling, *J. Am. Chem. Soc.*, **71,** 1930 (1949).
10. J. N. Atherton and A. M. North, *Trans. Faraday Soc.*, **58,** 2049 (1962).
11. A. M. North, *Polymer*, **4,** 134 (1963).
12. K. F. O'Driscoll, W. Wertz, and A. Husar, *J. Polym. Sci. A-1*, **5,** 2159 (1967).
13. S. Chiang and A. Rudin, *J. Macromol. Sci.-Chem.*, **A9**(2), 237 (1975).
14. S. Russo and S. Munari, *J. Macromol. Sci.-Chem.*, **A2**(7), 1321 (1968).
15. G. Bonta, B. M. Gallo, and S. Russo, *J. Chem. Soc. Faraday Trans. I*, **69,** 328 (1973).
16. M. Suzuki, H. Miyama, S. Fujimoto, *J. Polym. Sci.*, **31,** 212 (1958).
17. H. Miyama and S. Fujimoto, *J. Polym. Sci.*, **54,** 532 (1961).

Received September 26, 1977
Revised November 28, 1977